Scientific paper

Development of a Mathematical Model for the Dynamic Optimization of Batch Reactors, and MINLP Synthesis of Plug-flow Reactors in Complex Networks

Marcel Ropotar,[a,b]* Zdravko Kravanja[b]

[a] *Tanin Sevnica kemična industrija d.d., Hermanova cesta 1, 8290 Sevnica, Slovenia*

[b] *Faculty of Chemistry and Chemical Engineering, University of Maribor, P.O. Box 219, Maribor, Slovenia*

* *Corresponding author: E-mail: marcel.ropotar@uni-mb.si*

Received: 28-08-2007

Dedicated to the memory of professor Vojko Ozim

Abstract

This paper describes the development of a robust and efficient reactor model suitable for representing batch and plug-flow reactors (PFRs) in different applications. These would range from the nonlinear (NLP) dynamic optimization of a stand-alone batch reactor up to the mixed-integer nonlinear (MINLP) synthesis of a complex reactor network in overall process schemes. Different schemes for the Orthogonal Collocation on Finite Element (OCFE) and various model formulations, in the case of MINLP model, were studied in order to increase the robustness and efficiency of the model. A deterministic model for known kinetics was obtained for batch and PFR reactors and extended for uncertainties in process parameters and reaction kinetics when the kinetics is unknown. Different variations of the developed model were applied to certain problems, as examples. The first motivating example was the dynamic optimization of batch reactor and the second the MINLP synthesis of a process scheme for the production of allyl chloride. The NLP version of the model with moving finite elements was found to be the most efficient for representing a batch reactor in the dynamic optimization example, and PFR trains in the process synthesis example.

Keywords: Batch reactor, PFR reactor, orthogonal collocation, NLP, MINLP, process synthesis

1. Introduction

Kinetics in batch and PFR reactors is described using differential equations with time as independent variable in the case of batch reactors and retention time, reactor length or volume in the case of PFRs. These equations represent complex optimization problems, even in small and simple examples, because equation-oriented solvers cannot handle differential equations. The use of OCFE in optimization models of batch or PFR reactors has become a well-established numerical method. It is used to convert and approximate differential equations into a set of nonlinear algebraic equations in a variety of applications, ranging from dynamic optimization of a single stand-alone batch reactor up to MINLP synthesis of complex reactor networks in overall process schemes.

Over the last decade modelling, dynamic optimization, and on-line optimization have been the main research categories regarding the optimization of batch reactors. The modeling category is usually oriented towards a more realistic description of a batch reactor[1] and towards the use of special modeling techniques and strategies in cases of imperfect knowledge of kinetic studies involved, e.g. the use of tendency models[2] or a sequential experiment design strategy based on reinforcement learning.[3] The second category is related to more advanced aspects of dynamic optimization in respect of batch reactors, e.g. robust optimization of models, characterization by parametric uncertainty,[4] or stochastic optimization of multimodal batch reactors.[5] Finally in work relating to on-line optimization, which is currently the prevailing activity, different control schemes have been proposed, e.g.

feedforward/state feedback laws in the presence of disturbances and nonlinear state feedback laws for batch processes with multiple manipulated inputs have been developed.[6,7] Due to the complexity involved, dynamic optimization problems are regarded as difficult research tasks.

On the other hand, the synthesis of reactor networks in overall process schemes is even more complex because we are dealing with discrete (selection of units, connectivity, etc.) and continuous (temperatures, flows, pressures, etc.) decisions simultaneously, which give rise to complex high-combinatorial mixed-integer nonlinear problems. Several methods have been developed for solving MINLP problems and one of the more efficient is the outer approximation (OA) algorithm[8] and its extensions. It is also possible to solve MINLP reactor network synthesis problems using the geometrical approach,[9] based on the attainable region (AR) theory or even by more efficient hybrid approaches which combine both methods.[10] The geometrical approach, based on the AR theory, was first used for constructing an attainable region in the concentration space for 2-dimensional problems,[11] and then for multi-D problems.[12] Recently a novel concept of time-dependent Economic Regions (ERs) was incorporated into the MINLP synthesis of reactor networks within the overall process scheme.[13] ER is obtained when economic criteria (e.g. annual profit, cost) are plotted vs. volume, residence time, or some other variable in contrast to the Concentration Attainable Region (CAR), which is constructed using technological criteria (e.g. conversion, selectivity, yield).

A very important objective when optimizing reactor systems is to obtain reliable and feasible solutions, even in the presence of uncertain parameters. A lot of work has been carried out so far in design under uncertainty. For example, a novel approach was developed for the evaluation of design feasibility/flexibility, based on the principles of the deterministic global optimization algorithm α-BB[14] and a two-stage algorithm for design under uncertainty and variability was proposed.[15]

Efficiency when solving the above-mentioned reactor optimization problems depends significantly on the method applied to solve the embedded differential-algebraic systems of equation. From among different variations of OCFE methods, the one with fixed finite elements is the most straightforward and easiest for modeling batch and PFR reactors. However, when using fixed finite elements directly it is impossible to explicitly model the optimal retention times of the batch reactors nor the optimal outlet concentrations and conditions. Consequently, the use of flexible finite elements or moving finite elements is regarded as a conventional approach for overcoming these difficulties[16]. This model, however, seems to be more nonlinear because the length of the final element is converted into a variable.

The aim of this paper is to present the development of mathematical models suitable for optimization of batch and PFR reactors, which may either stand alone or be combined in complex reactor networks embedded within overall process flowsheets. Different schemes and strategies are applied to modelling and solving these dynamic and synthesis problems. The objective is to identify the most robust and efficient solution procedure.

2. Experimental – Numerical Procedure

The following four-step procedure was proposed for solving optimization problems that contain differential-algebraic systems of equation:

Simulation: During the first, optional step, simulation was performed using the MATHCAD professional package. The simulation is useful for preliminary analysis of a given kinetic system's behaviour, and to provide a good initial point for NLP or MINLP.

Model formulation: During the second step, a differential-algebraic optimization problem (DAOP) model was converted into an NLP or MINLP model. Differential equations were approximated into a set of nonlinear algebraic equations by the use of OCFE, and an integral term in the objective function was approximated by the Gaussian integration formula.

Solution: During the next step, either NLP or MINLP optimization was performed for the developed model.

Analysis: During the last step, sensitivity analysis was carried out by one-parametric NLP or MINLP optimization with production rate (demand) as a varying (uncertain) parameter. Sensitivity analysis can be upgraded for flexible dynamic optimization where uncertain parameters are included directly in the optimization. When process synthesis is carried out, ER can be constructed during this step, with reactor volume as varying parameter.

2. 1. Dynamic Optimization of Batch Reactor

Motivating example:

NLP and MINLP models for the optimization of batch and PFR reactors were developed, based on a motivating example of a batch reactor (Fig. 1), where consecutive reaction A → B → C is carried out and B is the desired product. Since the reaction is endothermic, the system can be heated and/or preheated. Whenever the optimal inlet temperature is higher than defined by the user the inlet must be preheated.

The kinetics of this reaction is the following:

$$\frac{\mathrm{d}c_\mathrm{A}}{\mathrm{d}t} = -k_0 \cdot \mathrm{e}^{\frac{-E_{\mathrm{a,A}}}{R \cdot T}} \cdot c_\mathrm{A}; \quad \frac{\mathrm{d}c_\mathrm{B}}{\mathrm{d}t} = k_0 \cdot \mathrm{e}^{\frac{-E_{\mathrm{a,A}}}{R \cdot T}} \cdot c_\mathrm{A} - k_0 \cdot \mathrm{e}^{\frac{-E_{\mathrm{a,B}}}{R \cdot T}} \cdot c_\mathrm{B}; \quad \frac{\mathrm{d}c_\mathrm{C}}{\mathrm{d}t} = k_0 \cdot \mathrm{e}^{\frac{-E_{\mathrm{a,B}}}{R \cdot T}} \cdot c_\mathrm{B}$$

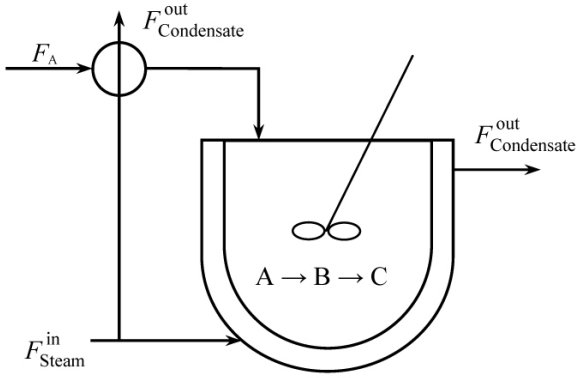

Figure 1: Batch reactor.

where c_A, c_B and c_C are concentrations of A, B, and C, respectively, k_0 is a pre-exponential constant, R universal gas constant, T reaction temperature, t time, and $E_{a,A}$ and $E_{a,B}$ are activation energies of both consecutive reactions.

The corresponding (DAOP) is given as follows:

$$\max Z = N_b \cdot \left[\sum_{p \in prod} C_p \cdot c_p V - \sum_{r \in react} C_r \cdot c_r V - C_{heat/cool} \left(\Phi_{preheat/precool} + \int_0^{t^{opt}} d\Phi_{heat/cool} dt \right) \right] \quad (1)$$

s.t.

$$\frac{dc_r}{dt} = -r_r \quad \forall r \in react \quad (2)$$

$$\frac{dc_p}{dt} = r_p \quad \forall p \in prod \quad (3)$$

$$\frac{dT}{dt} = -\sum_{p \in prod} \frac{\Delta_r H_p}{\rho \cdot c_p} \cdot (r_p) + \frac{\Phi_{heat/cool}(t)}{V \cdot \rho \cdot c_P} \quad (4)$$

$$\Phi_{preheat/precool} = (+/-)\rho \cdot V \cdot c_P \cdot (T_0 - T_b) \quad (5)$$

$$t \in [0, t^{opt}]; \; c_r, c_p, T, t, \Phi_{heat/cool}, \Phi_{preheat/precool} \geq 0 \quad \text{(DAOP)}$$

where c_r, c_p, r_r and r_p denote concentration and reaction rate for reactants and products, respectively, Z profit, N_b number of batches, C cost coefficients, t^{opt} optimal reaction time, T_0 inlet temperature, T_b desired temperature, $\Delta_r H$ reaction enthalpy, c_p specific heat capacity, ρ density of reactive mixture, $\Phi_{heat/cool}$ and $\Phi_{preheat/precool}$ heat-flow for heating/cooling and heat-flow for preheating/precooling, respectively. The objective is to maximize revenue for a certain number of batches. Costs for reactants and utilities are subtracted from the profit of the product sale (eq. (1)). Note that the cost function of the utility is integrated into the objective function over the whole time period. Eqs. (2) and (3) represent differential equations for the production rates of reactants and products, respectively, while eq. (4) is the differential equation for heat-flow. Heat-flow for preheating or precooling is calculated using eq. (5). The (DAOP) model for motivating example, shown above, cannot be used in equation-oriented solvers because they cannot handle differential equations. Therefore, the differential equations have to be converted into a set of nonlinear algebraic equations. In this way a (DAOP) model is converted into an NLP or MINLP model suitable for optimization. The OCFE method was applied to approximate the differential equations.

Below we present three variations of the OCFE method: i) one with fixed finite elements, ii) one with moving finite elements and iii) one with fixed but partly employed finite elements. Deterministic NLP and MINLP models for dynamic optimization of batch reactors were developed, based on these variations. In order to handle deviations of uncertain parameters, the deterministic models were upgraded with flexibility constraints. Thus, the flexible dynamic optimization models were finally developed.

2. 1. 1. NLP Model Formulation

Let us first describe the case of using the OCFE method with fixed and partly-employed finite elements. The following deterministic model (DFIX-NLP) was obtained, which is usually non-flexible or is flexible only for very small deviations of uncertain parameters:

$$\max_{t^{opt}, c_A, c_B, c_B, \Phi_{preheat}, \Phi_S} Z = \frac{28800}{t^{opt}_{tot} + 600} \cdot \left(C_1 c^{opt}_{B,l=NE} V - C_2 \cdot c^0_A V - C_3 \cdot c^{opt}_{C,l=NE} V - C_4 \cdot \Phi_{preheat} - C_5 \cdot \sum_{l=1}^{NE} \frac{t^{opt}_l}{2} \sum_{n=1}^{N} A_n \sum_{j=1}^{K} \Phi_{S,jl} \cdot \prod_{k=0, k \neq j}^{K} \frac{\frac{t^{opt}_l}{2}(x_n + 1) - t_{kl}}{t_{jl} - t_{kl}} \right) \quad (6)$$

s.t.

Residual equations for component balances:

$$\left. \begin{aligned} R_{B,il}(t_{il}) &= \sum_{j=0}^{K} c_{B,jl} \cdot \prod_{k=0, k \neq j}^{K} \frac{t_{il} - t_{kl}}{t_{jl} - t_{kl}} - k_0 \cdot e^{\frac{-E_{a,A}}{R \cdot T_{il}}} \cdot c_{A,il} + k_0 \cdot e^{\frac{-E_{a,B}}{R \cdot T_{il}}} \cdot c_{B,il} = 0 \\ R_{C,il}(t_{il}) &= \sum_{j=0}^{K} c_{C,jl} \cdot \prod_{k=0, k \neq j}^{K} \frac{t_{il} - t_{kl}}{t_{jl} - t_{kl}} - k_0 \cdot e^{\frac{-E_{a,B}}{R \cdot T_{il}}} \cdot c_{B,il} = 0 \end{aligned} \right\} \begin{aligned} &\forall i = 1,2,...K \\ &\forall l = 1,2,...NE \end{aligned} \quad (7)$$

$$\left.\begin{aligned}
&\left(c_{\mathrm{A}}^{0}-c_{\mathrm{A},il}\right)=\left(c_{\mathrm{B},il}-c_{\mathrm{B}}^{0}\right)+\left(c_{\mathrm{C},il}-c_{\mathrm{C}}^{0}\right)\\
&R_{T,il}(t_{il})=\sum_{j=0}^{K}T_{il}\cdot\prod_{k=0,k\neq j}^{K}\frac{t_{il}-t_{kl}}{t_{jl}-t_{kl}}+\frac{\Delta_{\mathrm{r}}H_{\mathrm{B}}}{\rho\cdot c_{p}}\cdot\left(k_{0}\cdot\mathrm{e}^{\frac{-E_{\mathrm{a,A}}}{R\cdot T_{il}}}\cdot c_{\mathrm{A},il}-k_{0}\cdot\mathrm{e}^{\frac{-E_{\mathrm{a,B}}}{R\cdot T_{il}}}\cdot c_{\mathrm{B},il}\right)+\\
&\frac{\Delta_{\mathrm{r}}H_{\mathrm{C}}}{\rho\cdot c_{p}}\cdot k_{0}\cdot\mathrm{e}^{\frac{-E_{\mathrm{a,B}}}{R\cdot T_{il}}}\cdot c_{\mathrm{B},il}-\frac{\Phi_{\mathrm{S},il}}{V\cdot\rho\cdot c_{p}}=0,
\end{aligned}\right\}\begin{aligned}&\forall i=1,2,...K\\&\forall l=1,2,...NE\end{aligned}\qquad(8)$$

where *N*, *K*, and *NE* are Gaussian quadrature points, collocation points and final elements, respectively.

Optimal outlet point is defined by Legendre polynomials:

$$\left.\begin{aligned}
&c_{\mathrm{B},l}^{\mathrm{opt}}\left(t_{l}^{\mathrm{opt}}\right)=\sum_{j=0}^{K}c_{\mathrm{B},jl}\cdot\prod_{k=0,k\neq j}^{K}\frac{t_{l}^{\mathrm{opt}}-t_{kl}}{t_{jl}-t_{kl}},\ T_{l}^{\mathrm{opt}}\left(t_{l}^{\mathrm{opt}}\right)=\sum_{j=0}^{K}T_{jl}\cdot\prod_{k=0,k\neq j}^{K}\frac{t_{l}^{\mathrm{opt}}-t_{kl}}{t_{jl}-t_{kl}}\\
&c_{\mathrm{C},l}^{\mathrm{opt}}\left(t_{l}^{\mathrm{opt}}\right)=\sum_{j=0}^{K}c_{\mathrm{C},jl}\cdot\prod_{k=0,k\neq j}^{K}\frac{t_{l}^{\mathrm{opt}}-t_{kl}}{t_{jl}-t_{kl}},\ \Phi_{\mathrm{S},l}^{\mathrm{opt}}\left(t_{l}^{\mathrm{opt}}\right)=\sum_{j=0}^{K}\Phi_{\mathrm{S},jl}\cdot\prod_{k=0,k\neq j}^{K}\frac{t_{l}^{\mathrm{opt}}-t_{kl}}{t_{jl}-t_{kl}}\\
&c_{\mathrm{A},l}^{\mathrm{opt}}=c_{\mathrm{A},i=0,l}-\left(c_{\mathrm{B},l}^{\mathrm{opt}}-c_{\mathrm{B}}^{0}\right)-\left(c_{\mathrm{C},l}^{\mathrm{opt}}-c_{\mathrm{C}}^{0}\right)
\end{aligned}\right\}\ \forall l=1,2,...NE\qquad(9)$$

Continuity conditions: the point at the interior knot is defined as the optimal interior point from the previous finite element defined by Legendre polynomials (eq. 9):

$$\left.\begin{aligned}
&c_{\mathrm{A},i=0,l}=c_{\mathrm{A},l-1}^{\mathrm{opt}}\qquad T_{i=0,l}=T_{l-1}^{\mathrm{opt}}\\
&c_{\mathrm{B},i=0,l}=c_{\mathrm{B},l-1}^{\mathrm{opt}}\qquad \Phi_{\mathrm{S},i=0,l}=\Phi_{\mathrm{S},l-1}^{\mathrm{opt}}\\
&c_{\mathrm{C},i=0,l}=c_{\mathrm{C},l-1}^{\mathrm{opt}}
\end{aligned}\right\}\ \forall l=2,3,...NE\qquad(10)$$

Equal time distribution:

$$t_{l}^{\mathrm{opt}}=t_{l-1}^{\mathrm{opt}}\qquad\forall l=2,3,...NE\qquad(11)$$

$$t_{\mathrm{tot}}^{\mathrm{opt}}=\sum_{l=1}^{NE}t_{l}^{\mathrm{opt}}\quad\forall l=1,2,...NE\qquad(12)$$

$$0\leq t_{l}^{\mathrm{opt}}\leq t_{l}^{\mathrm{opt,UP}}\quad\forall l=1,2,...NE\qquad(13)$$

(DFIX-NLP)

where A_n denotes coefficients for Gaussian integration formula, R_{B}, R_{C} and R_T residuals for B, C and *T*, respectively, t_{il} time variable for collocation point *i* and finite element *l*, t_l^{opt} optimal time of the finite element, and t_l^{opt} total optimal time. In order to equally distribute the load of numerical integration on the finite elements, all t_l^{opt} are set as equal, eq. (11). Total time is defined as a sum of all optimal times in all finite elements, eq. (12). Each fixed final element is defined as between zero and $t_l^{\mathrm{opt,UP}}$, eq. (13). Note that, since t_l^{opt} is continuously defined through the Legendre polynomials between the bounds, only part of the element is employed for integration (Fig. 2). It should also be noted that the profit and number of batches in the objective function (6) are defined for production covering 8 h and a 600 s non-operational period between batches. Thus, the number of batches is 28,880/(t_{tot}^{opt} + 600). On top of complexity from differential equations, additional complexity arises due to the presence of Gaussian numerical integral in the objective function where heat-flow is integrated over reaction time and which, in addition, is an optimization variable.

In the case when using OCFE with moving finite elements, additional nonlinearities of algebraic constraints are introduced in the model due to the presence of those variables which represent finite elements' lengths.

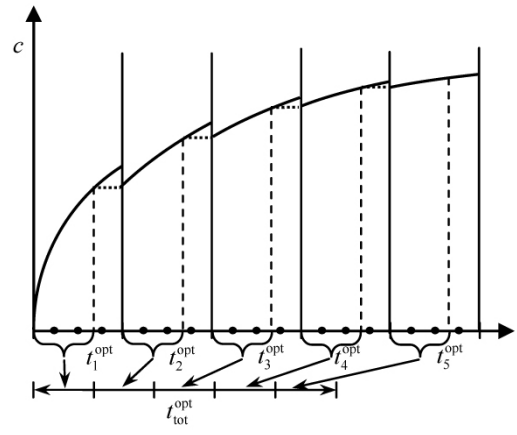

Figure 2: The graphical representation of 5 fixed and partly employed finite elements with 3 collocation points.

On the other hand, some nonlinearities vanish because optimal time is moved to the end of the finite element and several equations become linear. Note that, in contrast to the previous variation, entire finite elements are now employed for integration (Fig. 3). Since they have variable lengths, the elements are moving along the time. Some changes have to be made to the model (DFIX-NLP) in order to obtain a deterministic model with moving final elements (DMOV-NLP). Because t_l^{opt} is moved to the end of the final element it is replaced by finite element length ($\Delta\alpha_l$) and some terms are, therefore, simplified. The heatflow in the objective function is integrated over the whole length of the final element; consequently the objective function has the following form:

$$\max_{\alpha,c_A,c_B,c_B,\Phi_{\text{preheat}},\Phi_S} Z = \frac{28800}{t_{\text{tot}}^{\text{opt}} + 600} \cdot \left(\begin{array}{l} C_1 c_{B,l=NE}^{\text{opt}} V - C_2 \cdot c_A^0 V - C_3 \cdot c_{C,l=NE}^{\text{opt}} V - C_4 \cdot \Phi_{\text{preheat}} - \\ C_5 \cdot \sum_{l=1}^{NE} \frac{\Delta\alpha_l}{2} \sum_{n=1}^{N} A_n \sum_{j=1}^{K} \Phi_{S,jl} \cdot \prod_{k=0,k\neq j}^{K} \frac{\frac{1}{2}(x_n+1) - t_k}{t_j - t_k} \end{array} \right) \tag{14}$$

Also terms in the Legendre polynomials for calculating optimal outlet points, are simplified:

$$\left. \begin{array}{l} c_{B,l}^{\text{opt}}\left(t_l^{\text{opt}}\right) = \sum_{j=0}^{K} c_{B,jl} \cdot \prod_{k=0,k\neq j}^{K} \frac{1-t_k}{t_j - t_k}, \; T_l^{\text{opt}}\left(t_l^{\text{opt}}\right) = \sum_{j=0}^{K} T_{jl} \cdot \prod_{k=0,k\neq j}^{K} \frac{1-t_k}{t_j - t_k} \\ c_{C,l}^{\text{opt}}\left(t_l^{\text{opt}}\right) = \sum_{j=0}^{K} c_{C,jl} \cdot \prod_{k=0,k\neq j}^{K} \frac{1-t_k}{t_j - t_k}, \; \Phi_{S,l}^{\text{opt}}\left(t_l^{\text{opt}}\right) = \sum_{j=0}^{K} \Phi_{S,jl} \cdot \prod_{k=0,k\neq j}^{K} \frac{1-t_k}{t_j - t_k} \\ c_{A,l}^{\text{opt}} = c_{A,i=0,l} - \left(c_{B,l}^{\text{opt}} - c_B^0\right) - \left(c_{C,l}^{\text{opt}} - c_C^0\right) \end{array} \right\} \; \forall l = 1,2,...NE \tag{15}$$

All final elements are set as equal and total time is defined as a sum of the lengths of all finite elements:

$$\Delta\alpha_l = \Delta\alpha_{l-1} \quad \forall l = 2,3,...NE \tag{16}$$

$$t_{\text{tot}}^{\text{opt}} = \sum_{l=1}^{NE} \Delta\alpha_l \quad \forall l = 1,2,...NE \tag{17}$$

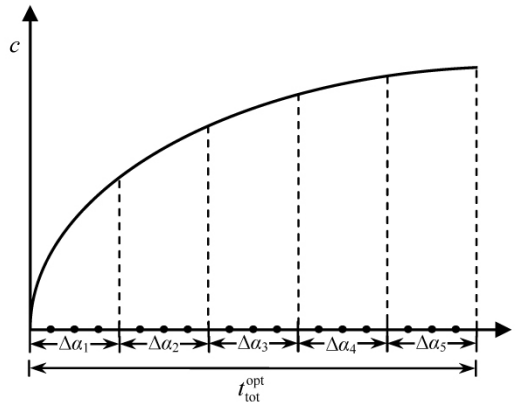

Figure 3: The graphical representation of 5 moving finite elements with 3 collocation points.

$$\Delta\alpha_l^{\text{LO}} \le \Delta\alpha_l \le \Delta\alpha_l^{\text{UP}} \quad \forall l = 1,2,...NE \tag{18}$$

Equations for residuals and continuity equations are the same as in the (DFIX-NLP) model (eq. (7), (8), (10)). (DMOV-NLP)

2. 1. 2. MINLP Model Formulation

Another variation when using OCFE, now with fixed finite elements, gives rise to a MINLP model, which is similar to the (DFIX-NLP) with the exception of some additional constraints while other equations are equal to those in (DFIX-NLP). Additional constraints are applied in order to select the optimal number of finite elements:

$$y_l \le y_{l-1} \quad \forall l = 2,3,...NE \tag{19}$$

$$t_l^{\text{opt}} \le t_l^{\text{opt,UP}} \cdot y_l \tag{20}$$

$$t_l^{\text{opt}} \le t_l^{\text{opt,UP}} + t^{\text{UP}} \cdot (1 - y_l) + t^{\text{UP}} \cdot (1 - y_{l+1}) \tag{21}$$

$$t_l^{\text{opt}} \ge t_l^{\text{opt,UP}} - t^{\text{UP}} \cdot (1 - y_l) - t^{\text{UP}} \cdot (1 - y_{l+1}) \tag{22}$$

$\forall l = 1,2,...NE$

where y_l denotes binary variable for finite element l. Ineq. (19) is applied to ensure that all finite elements up to the last selected one are, in fact, selected. If the corresponding finite element is rejected, ineq. (20) forces t_l^{opt} to zero. When the element is not the last one, ineqs. (21) and (22) are applied to force the t_l^{opt} of each finite element into the upper bound. Hence, all the selected finite elements are fully exploited for integration, except the last one where the optimal time is continuously defined by the Legendre polynomial between the element's bounds. Note that, in contrast to the NLP model where integration is distributed equally and continuously within all the finite elements, here integration is only applied to the selected finite elements. In the case of NLP optimization, the number of fi-

nite elements has to be set in advance and is, thus, usually overestimated in order to satisfy a given error tolerance, whereas, in MINLP cases, it is explicitly modelled in order to adjust it simultaneously to the minimal number of elements, during the optimization process.

In the case of the MINLP model, the robustness of the model was studied with respect to the use of different model formulations motivated by recently developed alternative convex-hull model formulation (ACH).[17] Namely a comparison was made between, Big-M formulation, conventional convex hull (CCH) and alternative convex hull formulation (ACH). In addition, the following representations of OAs in the solution point $\boldsymbol{x}^{\mathbf{k}}$ for the Outer Approximation/Equality Relaxation (OA/ER) algorithm were compared:

Big-M formulation:

$$h(\boldsymbol{x}^k)+\nabla_x h(\boldsymbol{x}^k)^{\mathrm{T}}\boldsymbol{x}-\nabla_x h(\boldsymbol{x}^k)^{\mathrm{T}}\boldsymbol{x}^k \le M(1-y)$$

CCH representation:

$$\nabla_x h(\boldsymbol{x}^k)^{\mathrm{T}}\boldsymbol{x} \le \left(\nabla_x h(\boldsymbol{x}^k)^{\mathrm{T}}\boldsymbol{x}^k - h(\boldsymbol{x}^k)\right)y$$

ACH representation:

$$\nabla_x h(\boldsymbol{x}^k)^{\mathrm{T}}\boldsymbol{x} \le \nabla_x h(\boldsymbol{x}^k)^{\mathrm{T}}\boldsymbol{x}^{\mathrm{f}} + \left(\nabla_x h(\boldsymbol{x}^k)^{\mathrm{T}}(\boldsymbol{x}^k-\boldsymbol{x}^{\mathrm{f}}) - h(\boldsymbol{x}^k)\right)y$$

Unlike CCH representation, where the continuous variables $\boldsymbol{x}$ are usually forced into zero values when the corresponding disjunctives are false, in ACH the variables are forced into arbitrarily-forced values, $\boldsymbol{x}^{\mathbf{f}}$.

Finally, in order to obtain better approximation of the OCFE method, additional inequality constraints for approximation error were included in the NLP and MINLP models (ineqs. (23)-(25)). These inequalities minimize the difference between values from the current finite element and the starting point of the next finite element

2. 1. 3. Flexible Dynamic Optimization

Different changes in operating conditions, costs, quality of raw material etc. could significantly affect the steady-state operation of the process and, hence, the desired amount and quality of the product. Such changing parameters are called uncertain parameters and processes which can tolerate these changes are regarded as flexible processes. For this reason, it is important to consider uncertainty, and hence flexibility, as additional constraints when obtaining flexible process solutions.

The main task of flexible design is to obtain optimally over-sized design variables for process equipment, which assure feasible solutions over the entire range of uncertain parameters using optimal investment costs. To ensure flexibility, besides nominal conditions, optimization has to be performed simultaneously at critical points, which is achieved by setting uncertain parameters at vertex points when the problem is convex. Thus, optimization at the critical vertex points serves as a flexibility constraint.

In this way the deterministic model was extended by the flexibility constraints, defined at all vertex points. This was done for all equations, inequalities, and state and control variables, except for design variables because they must correspond to all vertex points simultaneously. Consequently, the size of the process equipment is valid for every possible combination of uncertain parameters. Objective function was approximated at the nominal point. The model obtained is, therefore, $(N_{\mathrm{C}} + 1)$ times bigger than the deterministic model, where N_{C} is the number of vertex points. In the case with three uncertain parameters and eight vertex points, the model is nine-times larger vs. the Gaussian integration method with five quadrature points for continuous distributions for every uncertain parameter where the model would be 133 times bigger than the deterministic

$$-\varepsilon \le \sum_{j=0}^{K} c_{\mathrm{B},jl}\cdot\prod_{k=0,k\ne j}^{K}\frac{t_{il}-t_{kl}}{t_{jl}-t_{kl}} - k_0\cdot \mathrm{e}^{\frac{-E_{\mathrm{a,A}}}{R\cdot T_{0,l+1}}}\cdot c_{\mathrm{A},i=0,l+1} + k_0\cdot \mathrm{e}^{\frac{-E_{\mathrm{a,B}}}{R\cdot T_{i=0,l+1}}}\cdot c_{\mathrm{B},i=0,l+1} \le \varepsilon \tag{23}$$

$$-\varepsilon \le \sum_{j=0}^{K} c_{\mathrm{C},jl}\cdot\prod_{k=0,k\ne j}^{K}\frac{t_{il}-t_{kl}}{t_{jl}-t_{kl}} - k_0\cdot \mathrm{e}^{\frac{-E_{\mathrm{a,B}}}{R\cdot T_{i=0,l+1}}}\cdot c_{\mathrm{B},i=0,l+1} \le \varepsilon \tag{24}$$

$$-\varepsilon \le \sum_{j=0}^{K} T_{il}\cdot\prod_{k=0,k\ne j}^{K}\frac{t_{il}-t_{kl}}{t_{jl}-t_{kl}} + \frac{\Delta_{\mathrm{r}}H_{\mathrm{B}}}{\rho\cdot c_p}\cdot\left(k_0\cdot \mathrm{e}^{\frac{-E_{\mathrm{a,A}}}{R\cdot T_{i=0,l+1}}}\cdot c_{\mathrm{A},i=0,l+1} - k_0\cdot \mathrm{e}^{\frac{-E_{\mathrm{a,B}}}{R\cdot T_{i=0,l+1}}}\cdot c_{\mathrm{B},i=0,l+1}\right) +$$

$$\frac{\Delta_{\mathrm{r}}H_{\mathrm{C}}}{\rho\cdot c_p}\cdot k_0\cdot \mathrm{e}^{\frac{-E_{\mathrm{a,B}}}{R\cdot T_{i=0,l+1}}}\cdot c_{\mathrm{B},il+1} - \frac{\Phi_{\mathrm{S},i=0,l+1}}{V\cdot\rho\cdot c_p} \le \varepsilon \tag{25}$$

where ε is an error tolerance, e.g. 10^{-3}.

one. Therefore it is very useful, when no probability functions are known for uncertain parameters, to approximate objective function at a nominal point and, hence, very large model and expensive calculations are avoided. The following flexible model with moving finite elements (FMOV-NLP) was obtained where initial concentration of A, temperature, demand, pre-exponential factor and activation energy were defined as uncertain parameters:

Equal distribution of finite element lengths:

$$\Delta\alpha_{lu} = \Delta\alpha_{l-1,u} \tag{31}$$

$$D_u = \frac{28800}{t_{\mathrm{tot},u}^{\mathrm{opt}} + 600} \cdot \left(c_{\mathrm{B},l=NE,u}^{\mathrm{opt}} V_u \cdot M_{\mathrm{B}}\right) \tag{32}$$

$$V_{\mathrm{r}} \geq V_u$$

$$t_{\mathrm{tot},u}^{\mathrm{opt}} = \sum_{l=1}^{NE} \Delta\alpha_{lu} \; ; \; t_{\mathrm{tot}}^{\mathrm{opt}} \geq t_{\mathrm{tot},u}^{\mathrm{opt}} \tag{33}$$

$\forall u = 1,2,...N_{\mathrm{C}}+1$

(FMOV-NLP)

$$\max_{\substack{\alpha, c_{\mathrm{A}}, c_{\mathrm{B}}, \\ c_{\mathrm{B}}, \Phi_{\mathrm{preheat}}, \Phi_{\mathrm{S}}}} Z = \frac{28800}{t_{\mathrm{tot}}^{\mathrm{opt}} + 600} \cdot \left(\begin{array}{l} C_1 c_{\mathrm{B},l=NE}^{\mathrm{opt,N}} V^{\mathrm{N}} - C_2 \cdot c_{\mathrm{A}}^{0,\mathrm{N}} V^{\mathrm{N}} - C_3 \cdot c_{\mathrm{C},l=NE}^{\mathrm{opt,N}} V^{\mathrm{N}} - C_4 \cdot \Phi_{\mathrm{preheat}}^{\mathrm{N}} - \\ \dfrac{92993 \cdot V_{\mathrm{r}}^{0,128}}{10 \cdot 365} - C_6 \cdot \sum_{l=1}^{NE} \dfrac{\Delta\alpha_l^{\mathrm{N}}}{2} \sum_{n=1}^{N} A_n \sum_{j=1}^{K} \Phi_{\mathrm{S},jl} \cdot \prod_{k=0,k\neq j}^{K} \dfrac{\frac{1}{2}(x_n+1) - t_{kl}}{t_{jl} - t_{kl}} \end{array} \right) \tag{26}$$

Residual equations and component balances:

$$\left.\begin{array}{l} R_{\mathrm{B},ilu}(t_{ilu}) = \sum_{j=0}^{K} c_{\mathrm{B},jlu} \cdot \prod_{k=0,k\neq j}^{K} \dfrac{t_{ilu} - t_{klu}}{t_{jlu} - t_{klu}} - k_{0_u} \cdot \mathrm{e}^{\frac{-E_{\mathrm{a}_u,\mathrm{A}}}{R \cdot T_{ilu}}} \cdot c_{\mathrm{A},ilu} + k_{0_u} \cdot \mathrm{e}^{\frac{-E_{\mathrm{a}_u,\mathrm{B}}}{R \cdot T_{ilu}}} \cdot c_{\mathrm{B},ilu} = 0 \\ R_{\mathrm{C},ilu}(t_{ilu}) = \sum_{j=0}^{K} c_{\mathrm{C},jlu} \cdot \prod_{k=0,k\neq j}^{K} \dfrac{t_{ilu} - t_{klu}}{t_{jlu} - t_{klu}} - k_{0_u} \cdot \mathrm{e}^{\frac{-E_{\mathrm{a}_u,\mathrm{B}}}{R \cdot T_{ilu}}} \cdot c_{\mathrm{B},ilu} = 0 \end{array}\right\} \begin{array}{l} \forall i = 1,2,...K \\ \forall l = 1,2,...NE \\ \forall u = 1,2,...N_{\mathrm{C}}+1 \end{array}$$

Additional component balance:

$$\left(c_{\mathrm{A},u}^{0} - c_{\mathrm{A},ilu}\right) = \left(c_{\mathrm{B},ilu} - c_{\mathrm{B},u}^{0}\right) + \left(c_{\mathrm{C},ilu} - c_{\mathrm{C},u}^{0}\right) \tag{27}$$

Residual equations and energy balances:

$$R_{T,ilu}(t_{ilu}) = \sum_{j=0}^{K} T_{ilu} \cdot \prod_{k=0,k\neq j}^{K} \frac{t_{ilu} - t_{klu}}{t_{jlu} - t_{klu}} + \frac{\Delta_{\mathrm{r}} H_{\mathrm{B}}}{\rho \cdot c_p} \cdot \left(k_{0_u} \cdot \mathrm{e}^{\frac{-E_{\mathrm{a}_u,\mathrm{A}}}{R \cdot T_{ilu}}} \cdot c_{\mathrm{A},ilu} - k_{0_u} \cdot \mathrm{e}^{\frac{-E_{\mathrm{a}_u,\mathrm{B}}}{R \cdot T_{ilu}}} \cdot c_{\mathrm{B},ilu} \right) +$$

$$\frac{\Delta_{\mathrm{r}} H_{\mathrm{C}}}{\rho \cdot c_p} \cdot k_{0_u} \cdot \mathrm{e}^{\frac{-E_{\mathrm{a}_u,\mathrm{B}}}{R \cdot T_{ilu}}} \cdot c_{\mathrm{B},ilu} - \frac{\Phi_{\mathrm{S},ilu}}{V_u \cdot \rho \cdot c_p} = 0; \quad \forall i = 1,2,...K, \forall l = 1,2,...NE, \forall u = 1,2,...N_{\mathrm{C}}+1 \tag{28}$$

where additional index u is defined for N_{C} vertex points and the nominal point.

Optimal outlet point by Legendre polynomials:

$$\left.\begin{array}{l} c_{\mathrm{B},lu}^{\mathrm{opt}} = \sum_{j=0}^{K} c_{\mathrm{B},jlu} \cdot \prod_{k=0,k\neq j}^{K} \dfrac{1 - t_{ku}}{t_{ju} - t_{ku}}, \; T_{lu}^{\mathrm{opt}} = \sum_{j=0}^{K} T_{jlu} \cdot \prod_{k=0,k\neq j}^{K} \dfrac{1 - t_{ku}}{t_{ju} - t_{ku}} \\ c_{\mathrm{C},lu}^{\mathrm{opt}} = \sum_{j=0}^{K} c_{\mathrm{C},jlu} \cdot \prod_{k=0,k\neq j}^{K} \dfrac{1 - t_{ku}}{t_{ju} - t_{ku}}, \; \Phi_{\mathrm{S},lu}^{\mathrm{opt}} = \sum_{j=0}^{K} \Phi_{\mathrm{S},jlu} \cdot \prod_{k=0,k\neq j}^{K} \dfrac{1 - t_{ku}}{t_{ju} - t_{ku}} \\ c_{\mathrm{A},lu}^{\mathrm{opt}} = c_{\mathrm{A},i=0,lu} - \left(c_{\mathrm{B},lu}^{\mathrm{opt}} - c_{\mathrm{B},u}^{0}\right) - \left(c_{\mathrm{C},lu}^{\mathrm{opt}} - c_{\mathrm{C},u}^{0}\right) \end{array}\right\} \begin{array}{l} \forall l = 1,2,...NE \\ \forall u = 1,2,...N_{\mathrm{C}}+1 \end{array} \tag{29}$$

Continuity conditions:

$$\left.\begin{array}{l} c_{\mathrm{A},i=0,lu} = c_{\mathrm{A},l-1,u}^{\mathrm{opt}}, \; T_{i=0,lu} = T_{l-1,u}^{\mathrm{opt}}, \; c_{\mathrm{B},i=0,lu} = c_{\mathrm{B},l-1,u}^{\mathrm{opt}}, \\ \Phi_{\mathrm{S},i=0,lu} = \Phi_{\mathrm{S},l-1,u}^{\mathrm{opt}}, \; c_{\mathrm{C},i=0,lu} = c_{\mathrm{C},l-1,u}^{\mathrm{opt}} \end{array}\right\} \begin{array}{l} \forall l = 2,3,...NE \\ \forall u = 1,2,...N_{\mathrm{C}}+1 \end{array} \tag{30}$$

where D_u is the demand and reactor volume (V_r) is the largest volume of reactive mixture at all critical vertex points (V_u), eq. (33). Note that the objective function is approximated at the nominal point indicated by superscript N.

All the developed models were solved using a GAMS/CONOPT solver for NLP and a Mixed Integer Process SYNthesizer (MIPSYN), the successor of PROSYN-MINLP,[18] for MINLP dynamic problems.

2. 2. MINLP Synthesis of Reactor Networks in Overall Process Schemes

The three-step superstructure approach was applied for MINLP synthesis of a reactor network in an overall process scheme:

– definition of the reactor network superstructure within a process scheme,
– MINLP model formulation,
– solution of the MINLP problem.

2. 2. 1. Reactor Network Superstructure Within a Process Scheme

The superstructure by Iršič-Bedenik et al.[13] was applied (Fig. 4a). The reactor/separator superstructure comprises a sequence of PFR/continuous stirred tank reactors (CSTR) with side-streams and intermediate separators at different locations. Each PFR consists of a train (Fig. 4b) of several differential non-isothermal elements.

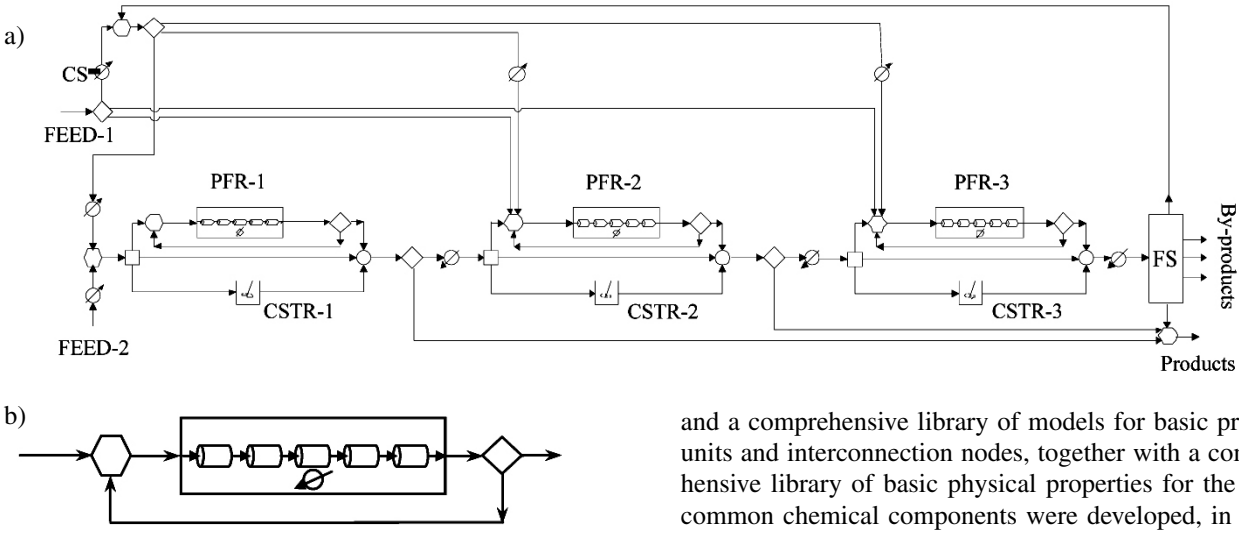

Figure 4: a) Superstructure of allyl chloride problem. b) Train of differential segments in PFR.

2. 2. 2. MINLP Model Formulation

In the next step, an MINLP model was developed for a given superstructure. Each segment was modelled individually and different variations of model for PFR were developed in analogy to the described dynamic models of a batch reactor. It should be noted that so far only MINLP model formulation for PFR trains with OCFE having fixed finite elements has been used because of better robustness of NLP with fixed than with moving finite elements.[13] The optimal number of elements was selected during MINLP optimization. Simultaneous heat integration was performed by Yee's model.[19] The overall model is highly nonlinear and nonconvex.

In this work the MINLP model for PFR trains was converted into an NLP model with moving finite elements, in order to reduce the combinatorial burden. Since the optimal length is now located at the end of the finite element, some equations become linear and, since the selection of the optimal final element is avoided, the combinatorial burden is significantly reduced.

2. 2. 3. Solution of the MINLP Problem

In the final step, the developed MINLP model was solved using a modified OA/ER algorithm,[18] which is an extension of the OA algorithm[8] and is implemented in the MIPSYN process synthesizer, the successor of PROSYN-MINLP.[18] MIPSYN enables automated execution of simultaneous topology, and parameter optimization of the processes. Optimization of each NLP subproblem is performed only on existing units, rather than on the entire superstructure, which substantially reduces the sizes of the NLP subproblems. An NLP initializer, model generator and a comprehensive library of models for basic process units and interconnection nodes, together with a comprehensive library of basic physical properties for the most common chemical components were developed, in order to facilitate the modelling and solution procedure.

Sensitivity analysis can be performed and ER can be constructed during the solution step. If in the AR, technological criteria such as conversion, selectivity or yield are drawn in a concentration space, we call such regions CAR. In order to reflect economic criteria, annual profit or annual cost can be plotted vs. reactor volume, retention time or some other variable, for different reactor systems. ERs can thus be constructed and their boundaries identi-

fied using the most economically-optimal reactor systems.

3. Results and Discussion

3. 1. Example 1 – Dynamic Optimization of Batch Reactor

A motivating example was modelled, as described in 2.1., and solved with GAMS, using data shown in Table 1.

Table 1: Data for example 1.

Data	R	k_0	$\Delta_r H_A$	$\Delta_r H_B$	ρ	$E_{a,A}$	$E_{a,B}$	c_p	V
Value	8.314	32500	50	50	700	46000	53000	1.5	0.8
Unit	J (mol K)$^{-1}$	(mol s)$^{-1}$	kJ mol^{-1}	kJ mol^{-1}	kg m^{-3}	J mol^{-1}	J mol^{-1}1	kJ (kg K)$^{-1}$	m^3

3. 1. 1. Deterministic Dynamic Optimization of a Batch Reactor

Table 2 shows results for NLP and MINLP models with fixed finite elements and NLP and MINLP models with moving finite elements. The last two columns outline NLP and MINLP solutions obtained by considering approximation error tolerance $\varepsilon = 10^{-3}$.

Table 2: Comparison among different models.

model	NLP (fixed FE)	MINLP (fixed FE)	NLP (moving FE)	NLP ($\varepsilon = 10^{-3}$) (moving FE)	MINLP ($\varepsilon = 10^{-3}$) (fixed FE)
c_A^{opt} /mol L^{-1}	0.101	0.101	0.101	0.101	0.101
c_B^{opt} /mol L^{-1}	0.605	0.605	0.605	0.607	0.605
c_C^{opt}mol L^{-1}	0.094	0.094	0.094	0.092	0.094
T^{opt}/K	369.1	369.3	369.3	369.2	369.3
t^{opt}/s	142.55	138.69	139.95	173.65	139.85
Z/k$	36.996	37.024	36.998	36.574	36.999
t_{CPU}/s	11.46	244.48	7.07	33.96	337.88

It can be seen that the solutions are very similar: small differences occur in temperatures, total optimal time, and profit. However, the CPU time (t_{CPU}) for solving the NLP model is significantly smaller than for the MINLP because 6 major MINLP iterations have to be performed in order to obtain an optimal solution. However, annual profits obtained using the MINLP model are somewhat grater than for the NLP. It can be seen, moreover, that the NLP model with moving finite elements requires somewhat less CPU time than the one with fixed final elements. With 50 finite elements, the MINLP and NLP model were able to tolerate an approximation error tolerance of less than 10^{-3}. When approximation error tolerance is explicitly considered in the model, the value of the objective function is, as expected, somewhat smaller. Both solutions are very similar for almost all process parameters. The only difference concerns temperature profiles where the temperature profile from the NLP solution is approximately 10 K's lower than the MINLP temperature profile, leading to significantly longer optimal time (173.65 vs. 139.85). It should be noted that Big-M model formulation was used in the case of MINLP.

Time-dependent profiles were obtained as a result of dynamic optimization. The concentration profiles are shown in Figure 5 for that NLP with moving finite elements in Table 2. It can be seen how concentrations of B and C increase and concentration of A decreases with time.

Comparison between three different MINLP model formulations is given in Table 3. It can be seen that, when fixed final elements were used, the t_{CPU} needed for solving 11 major iterations is comparable with Big-M and CCH formulations, while against ACH formulation it is somewhat smaller. A slightly better solution was found with Big-M formulation; otherwise the results are very similar.

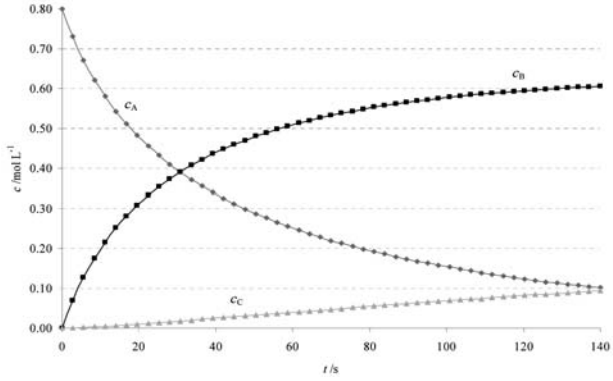

Figure 5: Concentration profiles for example 1.

In addition, sensitivity analysis was performed for the batch reactor. Temperatures were taken as varying parameters and, as a result, curves for the selectivity of

Table 3: Comparison among three different model formulations.

Process parameter	MINLP formulation		
	a) BIG-M (fixed FE)	b) CCH (fixed FE)	c) ACH (fixed FE)
c_A^{opt} /mol L^{-1}	0.101	0.101	0.101
c_B^{opt} /mol L^{-1}	0.605	0.605	0.605
c_C^{opt}mol L^{-1}	0.094	0.094	0.094
T^{opt}/K	369.3	369.3	369.3
t^{opt}/s	138.69	139.85	139.85
Z/k$	37.024	36.999	36.999
t_{CPU}/s	627.26	639.21	844.09

B and the production rate were obtained, respectively (Fig. 6).

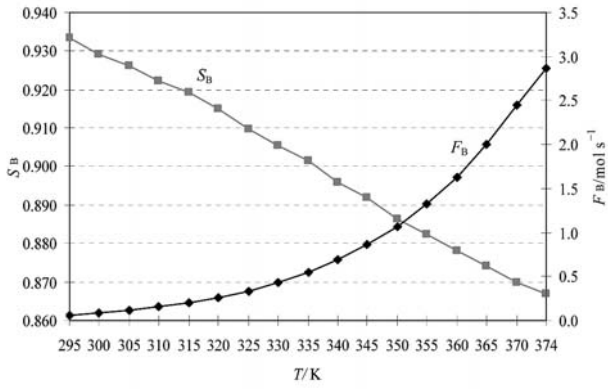

Figure 6: A trade-off between selectivity and production rate.

3. 1. 2. Flexible Dynamic Optimization of a Batch Reactor

A flexible model (FMOV-NLP) was applied for uncertain parameters: inlet temperature, inlet concentration and demand, and in addition for the pre-exponential factors and activation energies of both reactions. Values of uncertain parameters in vertex and nominal points are given in Table 4.

Table 4: Values of uncertain parameters in vertex and nominal points.

Parameter	c_A^{in}/mol L^{-1}	T^{in}/K	D/t d^{-1}	k_0/s^{-1}	$E_{a,A}$/J mol^{-1}	$E_{a,B}$/J mol^{-1}
θ^{LO}	0,6	360	1,4	27500	43000	50000
θ^{N}	0,8	380	1,9	32500	46000	53000
θ^{UP}	1,0	400	2,4	37500	49000	56000

A deterministic model (DMOV-NLP) was applied for the deterministic design (Table 5a) and a flexible model (FMOV-NLP) for flexible design with 3 (c_A^{in}, T^{in}, D in Table 5b) and 6 (c_A^{in}, T^{in}, D, k_0, $E_{a,A}$, $E_{a,B}$ in Table 5c) uncertain parameters combining into 8 and 64 vertex points, respectively.

It can be seen from Table 5 that profit from the flexible solution is, as expected, somewhat lower because of a higher investment costs for an optimally over-sized reactor. Higher reactor volume does not mean higher production of B, since it is limited by the current values of changeable product demand, considered as an uncertain parameter. However, the reactor has to be over-sized in order to satisfy higher demand or other deviations. When the kinetics of the reactions is also considered as uncertain, it has a significant influence on the reactor volume, which doubles in order to tolerate the specified deviations of uncertain parameters. If t_{CPU} are compared, it can be seen that flexible optimization increases the required computational effort, especially in the case of 6 uncertain parameters with 64 vertex points where an hour and a half of CPU time was required.

Table 5: Results for deterministic and flexible design with 3 and 6 uncertain parameters.

Process parameter	Design		
	a) deterministic	b) flexible 3 uncertain parameters	c) flexible 3 uncertain parameters
c_A^{opt} /mol L^{-1}	0.082	0.082	0.082
c_B^{opt} /mol L^{-1}	0.624	0.624	0.624
c_C^{opt}mol L^{-1}	0.094	0.094	0.094
T^{opt}/K	345.8	345.8	345.8
t^{opt}/s	411.08	411.36	411.55
Vr/m3	1.069	1.275	2.380
Z/k$	42.505	42.488	42.426
t_{CPU}/s	3.34	193.36	5745.77

3. 2. Example 2 – The MINLP Synthesis of a Reactor Network in the Overall Process Scheme

Using the superstructure approach, as described in 2.2., a process synthesis example regarding the production of allyl chloride was used, with basic data as shown in Table 6. A description of the process is given elsewhere.[13] All three different MINLP model formulations (Big-M, CCH, and ACH) were applied for the process superstructure of Fig. 4a and solved by MIPSYN where the PFR trains (Fig. 4b) are represented by the i) MINLP model with fixed finite elements, and the ii) NLP model with moving finite elements. The objective is to maximize net present value (V_{NP}) for a period of ten years. The results until 11 major iterations are given in Table 7.

Table 6: Data for example 2.

Reaction	k_0	E_a/J mol^{-1}
A + Cl_2 → B + HCl	1.5 10^{-6} s^{-1}	66271
B + Cl_2 → C + HCl	4.4 10^{8} s^{-1}	99410
A + Cl_2 → D	100 L (mol s)$^{-1}$	33140

A: propene; B: allyl chloride; C: 1,3-dichloropropene; D: 1,2-dichloropropane

Table 7: Results for allyl chloride example.

MINLP formulation	PFR train model formulation			
	MINLP		NLP	
	V_{NP}/k$	t_{CPU}/s for 11 it.	V_{NP}/k$	t_{CPU}/s for 11 it.
Big-M	81,924	84	82,332	51
CCH	82,068	165	81,979	382
ACH	81,769	235	81,780	101

As can be seen from Table 7, t_{CPU} decreased when the NLP model was used for PFR trains except in the case of CCH formulation. This is clearly emphasized in the case of ACH model formulation where t_{CPU} using the NLP model for PFR trains is more than two times smaller than when using the MINLP model. In the case of Big-M formulation, a better solution was found using the NLP model for PFR trains.

3. 2 . 1. Sensitivity analysis and definition of an Economic Region:

Any change in V_{NP} vs. reactor volume was investigated using sensitivity analysis. One-parametric MINLP optimization, with reactor volume as varying parameter, was performed directly for all three model formulations, in order to construct ER (Fig. 7). The obtained optimal structure and V_{NP} for each volume, is given in Table 8. The best solution among all three formulations is marked for each volume. All these best solutions plus the best one from Table 7 define the border of ER in Figure 7.

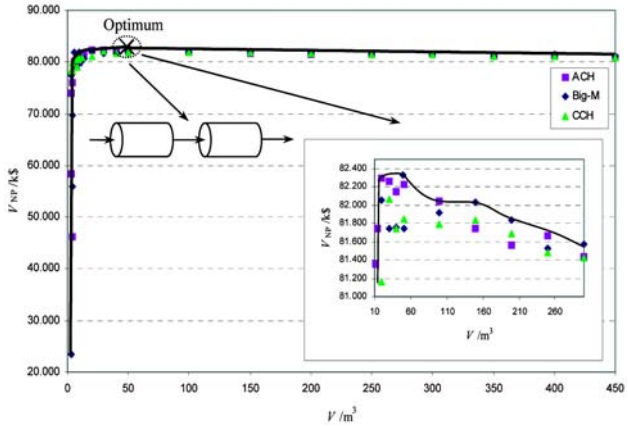

Figure 7: ER for allyl chloride example.

Table 8: Optimal structure for all three formulations.

V	Big – M		CCH		ACH		Border of ER	
	V_{NP} /k$	Optimal structure	V_{NP} /k$	Optimal structure	V_{NP} /k$	Optimal structure	V_{NP} /k$	Optimal structure
3	23,534	2,3	78,512	2,3,5	58,430	2,3	78,512	2,3,5
3.5	77,328	2,3,5	78,317	1,3	74,051	2,3	78,317	1,3
3.75	69,787	1,4,5	78,304	2,4,5	46,242	2,3	78,304	2,4,5
4	55,998	1,4,5	79,854	2,3,5	76,034	2,4,5	79,854	2,3,5
6	81,870	1,3,5	80,708	1,3,5	80,137	2,4,5	81,870	1,3,5
7	81,503	1,3	80,479	2,4,5	79,283	1,3,5	81,503	1,3
8	79,489	1,4,5	79,036	1	80,318	2,3	80,318	2,3
9	81,318	2,3	80,370	2,4,5	80,772	2,4,5	81,318	2,3
10	81,879	1,3	80,752	2,3	79,845	1	81,879	1,3
12	80,331	2,3	80,876	2,4,5	81,361	2,3	81,361	2,3
14	80,639	1	80,973	2,4,5	81,744	2,3	81,744	2,3
20	82,053	1,3	81,160	1	82,295	1,3	82,295	1,3
30	81,742	2,3,5	82,063	2,3,5	82,264	1,3	82,264	1,3
40	81,761	1	81,746	1	82,150	1,3	82,150	1,3
49	82,332	1,3	/		/		82,332	1,3
50	81,739	2,3	81,850	1	82,227	2,3,5	82,227	2,3,5
100	81,919	1	81,787	2,3	82,043	1,3	82,043	1,3
150	82,028	2,3	81,840	1	81,745	1,3	82,028	2,3
200	81,830	1,3	81,686	1	81,562	1,4,5	81,830	1,3
250	81,529	1	81,477	2,3	81,665	1,4,5	81,665	1,4,5
300	81,572	1,3	81,420	1	81,438	2,3	81,572	1,3
350	81,112	1,4,5	81,105	1	81,027	1,3	81,112	1,4,5
400	81,384	2,3	81,164	1	81,350	2,3	81,384	2,3
450	81,022	1	80,954	1	80,933	1	81,022	1

Binary number: 1 – PFR-I, 2 – CSTR-I, 3 – PFR-II , 4 – CSTR-II, 5 – PFR-III, 6 – CSTR-III

Note that the best solution was found when using MINLP optimization and Big-M formulation (Table 7), and is marked in Figure 7. It is interesting to note that optimal structures differ significantly from one volume to another. This is most likely due to strong nonlinear and discrete interaction between the reaction, separation and utility subsystems in the process scheme.

4. Conclusions

The main goal of the research was to obtain robust and efficient NLP or MINLP models, suitable for solving different applications ranging from dynamic optimization of batch reactors up to the MINLP synthesis of reactor networks with PFR reactors, in overall process schemes.

An efficient four-step numerical solution procedure was proposed and NLP and MINLP models were developed based on motivating examples where different OCFE schemes were applied in order to develop robust and efficient reactor models. Furthermore, different model formulations were studied in the case of the MINLP model.

Two examples were solved. The NLP model with moving finite elements was the most efficient in the case of a batch reactor's dynamic optimization because nonlinearities were reduced and CPU time also decreased. In order to handle uncertainties, the deterministic NLP model was extended by flexibility constraints. A flexible model was obtained in this way. This model can tolerate deviations in process conditions and in the kinetics of the reaction. In the case of the MINLP model, Big-M formulation was the most efficient because it comprises the smallest number of variables and equations.

Because the NLP model with moving finite elements was the most efficient in the dynamic optimization example, it was also applied to the process synthesis example of allyl chloride production, for modeling the PFR trains. When the NLP model was used for PFR trains, rather than the MINLP, CPU time was decreased, especially in the case of ACH. Sensitivity analysis with one-parametric MINLP optimization was performed for all three formulations and the border of the ER was constructed directly from the best solutions. The ER indicates high variations for the reactor system's optimal structure versus the reactor volume over the whole range of the reactor's volume. On the other hand, the V_{NP} changes rapidly only at smaller reactor volumes. At larger volumes, the border of ER becomes more smooth indicating the existence of many similar non-optimal solutions.

Optimization of a complex industrial application is presently under way based on the experience gained from this research.

6. Acknowledgment

The authors are grateful to the Slovenian Ministry of Higher Education, Science and Technology for financial support (PhD research fellowship contract No. 3211-05-000566).

6. References

1. J. M. Zaldivar, H. Hernandez, C. Barcons, *Thermochim. Acta* **1996**, *289,* 267–302.
2. J. Fotopoulos, C. Georgakis, H. G. Stenger, *Chem. Eng. Process.* **1998**, *37,* 545–558.
3. E. C. Martinez, *Comput. Chem. Eng.* **2000**, *24,* 1187–1193.
4. D. Ruppen, C. Benthack, D. Bonvin, *J. Process Control* **1995**, *5,* 235–240.
5. E. F. Carrasco, J. R. Banga, *Ind. Eng. Chem. Res.* **1997**, *36*, 2252–2261.
6. S. Rahman, S. Palanki, *AICHE J.* **1996**, *42*, 2869–2882.
7. S. Rahman, S. Palanki, *Comput. Chem. Eng.* **1998**, *22*, 1429–1439.
8. M. A. Duran, I. E. Grossmann, *Math. Program.* **1986**, *36,* 307–339.
9. A. Lakshmanan, L.T. Biegler, *Ind. Eng. Chem. Res.* **1996,** *35*, 1344–1353.
10. N. Iršič Bedenik, B. Pahor, Z. Kravanja, *Comput. Chem. Eng.* **2004**, *28,* 693–706.
11. D. Hildebrandt, L. T. Biegler, *AICHE Symp. Ser.* **1995**, *305*, 52–67.
12. M. Feinberg, D. Hildebrandt, *Chem. Eng. Sci.* **1997**, *52*, 1637–1665.
13. N. Iršič Bedenik, M. Ropotar, Z. Kravanja, *Comput. Chem. Eng.* **2007**, *31,* 657–676.
14. C. A. Floudas, Z. H. Gümüş, M. G. Ierapetritou, *Ind. Eng. Chem. Res.* **2001,** *40*, 4267–4282.
15. W. C. Rooney, L. T. Biegler, *AICHE J.* **2003**, *49*, 438–449.
16. J. E. Cuthrell, L. T. Biegler, *Comput. Chem. Eng.* **1989**, *13*, 49–62.
17. M. Ropotar, Z. Kravanja, (2006), *Implementation of efficient logic-based techniques in the MINLP process synthesizer MIPSYN*, in: W. MARQUARDT, C. PANTELIDES (eds.), 16th European symposium on computer aided process engineering and 9th International symposium on process systems engineering. Part A, (Computer-aided chemical engineering, 21A). Amsterdam [etc.]: Elsevier, cop., *16th European symposium on computer aided process engineering and 9th International symposium on process systems engineering,* Garmisch-Partenkirchen, Germany, pp. 233–238.
18. Z. Kravanja, I. E. Grossmann, *Comput. Chem. Eng.* **1994**, *18,* 1097–1114.
19. T. F. Yee, I. E. Grossmann, *Comput. Chem. Eng.* **1990**, *14,* 1165–1184.

Nomenclature

A_n	Coefficient for Gaussian integration formula,	/
c	Concentration;	mol L^{-1}
c_A^{in}	Inlet concentration of reactant A;	mol L^{-1}
C	Cost coefficient;	k$
c_P	Specific heat capacity;	kJ $(molK)^{-1}$
D	Demand of the product;	t d^{-1}
E_a	Activation energy;	J mol^{-1}
F_B	Production rate;	mol s^{-1}
$h(\boldsymbol{x})$	Equality nonlinear constraint function;	/
$\Delta_r H$	Reaction enthalpy;	kJ mol^{-1}
k_0	Pre-exponential constant;	$(mols)^{-1}$
M	Molar mass;	kg $kmol^{-1}$
N_b	Number of batches;	/
N_C	Number of vertex points;	/
r	Reaction rate;	mol m^{-3} s^{-1}
R	Universal gas constant;	J $(molK)^{-1}$
S_B	Selectivity;	/
t	time;	s
t_{CPU}	CPU time;	s
t_{tot}^{opt}	Total optimal time;	s
T	Temperature;	K
V	Volume;	m^3
V_{NP}	Net present value;	k$
$\boldsymbol{x}$	Vector of variables;	/
$\boldsymbol{x}^f$	Vector of arbitrarily-forced values;	/
$\boldsymbol{x}^k$	Vector of solutions;	/
y	Binary variable;	/
Z	Profit;	k$
Δa	One-dimensional variable;	/
ε	Error tolerance;	/
ρ	Density;	kg m^{-3}
Φ	Energy flow rate;	kW

Superscripts

k	Solution
LO	Lower
N	Nominal point
opt	Optimal
UP	Upper

Subscripts

A	Reactant A
B	Product B
C	By-product C
heat/ cool	Heating/Cooling
i, j, k	Collocation points
l	Finite element
n	Points for Gaussian integration formula
p	Product
preheat/ precool	Preheating/precooling
r	Reactant
s	Steam
u	Vertex point

Povzetek

Razvili smo učinkovit model za reaktor, ki je primeren za modeliranje šaržnih in cevnih reaktorjev. Uporabimo ga lahko za nelinearno (NLP) dinamično optimiranje šaržnega reaktorja kot posamične procesne enote ali za mešano celoštevilsko (MINLP) sintezo kompleksnih reaktorskih omrežij v celotni procesni shemi. Da bi povečali robustnost in učinkovitost modela, smo proučevali različne sheme in strategije za ortogonalno kolokacijo končnih elementov in v primeru MINLP modela tudi različne modelne formulacije. Dobili smo deterministični model z znano kinetiko za šaržne in cevne reaktorje. Razširili smo ga za pogoje nedoločenosti v procesnih parametrih in reakcijski kinetiki v primeru, ko je kinetika neznana. Različne variante razvitega modela smo uporabili na dveh primerih. Prvi primer je bil motivacijski primer dinamičnega optimiranja šaržnega reaktorja in drugi MINLP sinteza procesne sheme proizvodnje alilklorida. NLP model s pomičnimi končnimi elementi se je izkazal za najbolj učinkovitega tako pri optimiranju šaržnega reaktorja kot pri cevnem reaktorju v procesni sintezi.